Available online at www.sciencedirect.com

ScienceDirect

Geochimica et Cosmochimica Acta 316 (2022) 59–68

Geochimica et Cosmochimica Acta

www.elsevier.com/locate/gca

An internal energy-dependent model for the Grüneisen parameter of silicate liquids

Yacong (Brooke) Zhou [a], William A. Goddard [a], Paul D. Asimow [b,*]

[a] Division of Chemistry and Chemical Engineering, California Institute of Technology, Pasadena, CA, USA
[b] Division of Geological and Planetary Sciences, California Institute of Technology, Pasadena, CA, USA

Received 22 March 2021; accepted in revised form 4 October 2021; Available online 13 October 2021

Abstract

We investigated the accuracy of the Mie-Grüneisen approximation, which treats the Grüneisen parameter (γ) as a one-parameter function of volume, for use in describing the thermal equation of state of a silicate liquid. For this study, we focused on a single composition: the diopside-anorthite eutectic, an Fe-free basalt analog that has been extensively studied by shock wave experiments. We tuned an empirical force-field to a small set of *ab initio N-V-T* molecular dynamics simulations to ensure that it reproduces pressure, heat capacity, and γ at high and low pressures. We then used empirical force-field molecular dynamics simulations in a larger system and for longer run times to ensure accurate extraction of γ at numerous *N-V-E* state points. To first order, the results show the expected volume-dependence for silicate liquids, with γ increasing as volume decreases. However, there are also significant and systematic variations of γ with internal energy (E) at constant volume. We propose a simple model form that captures the volume and E dependence of γ with only one more free parameter than a typical Mie-Grüneisen formulation. We demonstrate the utility of this new model for well-constrained fitting to sparse shock wave experiment data below 200 GPa, obtaining a marked improvement in the ability to simultaneously fit the pre-heated liquid Hugoniot and points substantially offset from this Hugoniot.

Keywords: Molecular dynamics; Silicate liquids; Grüneisen parameter; Equation of state

1. INTRODUCTION

Silicate liquids form by melting of the rocky parts of terrestrial planets and — due to their buoyancy, mobility, and tendency to strongly fractionate chemical elements — become the main agents of differentiation and evolution of planetary mantles and crusts (Trønnes et al., 2019; Halliday et al., 2001; Boyet et al., 2003; Hofmann, 1988). Understanding the roles of silicate liquids in the early and ongoing chemical and dynamical evolution of the Earth and other planets requires first knowing when and where melting occurs (Nakajima and Stevenson, 2015; Tonks and Melosh, 1993; de Vries et al., 2016), but also calls for detailed knowledge of the physical properties of such liquids (Labrosse et al., 2007; O'Rourke, 2020; Stixrude et al., 2009), in order to trace the mass, momentum, and energy transfers accompanying their freezing. Essential properties include transport properties such as viscosity and diffusivity, but here we focus on the equation of state (EOS), i.e., the relationship among specific volume (V, the reciprocal of density), pressure (P), and either temperature (T) or internal energy (E). The EOS directly predicts the buoyancy of the liquid, and hence the driving force for upwards or downwards motion relative to coexisting solids under the influence of gravity. At the same time, the EOS also provides an essential ingredient of any polybaric thermodynamic model (since V is the pressure derivative of Gibbs free energy at constant T). Many EOS formulations

* Corresponding author.
E-mail address: asimow@caltech.edu (P.D. Asimow).

https://doi.org/10.1016/j.gca.2021.10.005
0016-7037/

are defined by decomposition into a reference path through P-V space (such as an isotherm, isentrope, or Hugoniot) and a thermal pressure term that governs offsets to hotter or colder states than those along the reference path. In turn, the most widely used formulations of the thermal pressure are expressed in terms of the Grüneisen parameter $\gamma = V\left(\frac{\partial P}{\partial E}\right)_V$. One key reason for the use of γ is the accuracy, in solid phases, of the Mie-Grüneisen approximation, which holds that γ is approximately a one-parameter function of volume. This is convenient because the thermal pressure term at constant volume then takes the form of a finite difference instead of an integral. Some studies have noted that this approximation is not perfect even for solids (Zhang et al., 2019), but in this work we focus on whether the approximation is justified for silicate liquids and propose an extension for more accurate formulation of the liquid EOS.

In the early 20th century, the Mie-Grüneisen model was derived from a high-temperature hard-sphere model of a crystal by Mie (1903) and was extended to temperatures below the Debye temperature by Grüneisen (1912). In solids, γ typically decreases with decreasing volume upon compression. The Mie-Grüneisen model is motivated by the essential role of phonons, or atomic vibrations, in the thermal expansion of solids and by the quasiharmonic approximation (Holzapfel, 2005; Bertoldi et al., 2014). Nevertheless, the compact functional form of the Mie-Grüneisen thermal pressure has also motivated its use in liquid equations of state. The concept was first introduced by Knopoff and Shapiro (1970) and subsequently widely adopted (Arp et al., 1984). One notable development in thinking about γ in silicate liquids came via ultrasonic data at high pressure (Boehler and Ramakrishnan, 1980), shock wave experiments (Brown et al., 1987, 2007, 2009, 2013), and molecular dynamics simulations (Stixrude and Karki, 2005; De Koker, 2010; Spera et al., 2011). These studies all showed that γ behaves differently in silicate liquids and solids under compression, with γ (viewed as a function only of volume) universally increasing with decreasing volume in liquids. Several theories have been put forward to explain this behavior, appealing to changes in the mean coordination number of the cations (Stixrude et al., 2009), to free-volume or entropy effects (Jing and Karato, 2011), or both (Wolf et al., 2015).

Although the Mie-Grüneisen approximation lacks theoretical justification in the case of liquids, there has been limited study of the deviations of γ in silicate liquids from a strict one-parameter dependence on volume. In fact, molecular dynamics simulations of numerous pure liquids reveal systematic deviations from the Mie-Grüneisen approximation (Mausbach et al., 2016). Commonly, γ increases with increasing T (or E) at constant volume when the volume is large, but decreases with increasing T (or E) at constant volume when the volume is small. This behavior is also present in two previous molecular dynamics studies of the silicate liquid composition $CaAl_2Si_2O_8$ (anorthite) – both the *ab initio* study of De Koker (2010) and the empirical force-field study of Ghiorso et al. (2009), though the authors of these studies did not comment on this behavior.

Shock-wave experiments using gas-guns, lasers, or magnetically driven compression are the main experimental approaches to characterizing the EOS of liquid silicates at pressures relevant to deep planetary interiors. These experiments determine γ indirectly (from finite differences among $P - V - E$ state points or from sound speed measurements) and only at certain state points along the Hugoniot. They do not yet have the precision to directly test whether γ has a non-negligible temperature dependence at constant volume in silicate liquids under mantle conditions. Hence molecular dynamics (MD) calculations take on an important role in identifying the functional dependence and suggesting functional forms that can then be fitted to the relatively sparse constraints from shock wave experiments. MD studies of liquids have distinctive computational challenges: liquids lack long-range atomic order that might reduce the computation to a small unit cell, natural silicate liquids occupy a complex multicomponent compositional space, and the relevant temperatures for planetary mantles impose slow atomic velocities that require long and computationally expensive run durations to ensure ergodicity. For these reasons, both *ab initio* and empirical simulation are competitive approaches to the study of silicate liquids. The ability to simulate many more atoms for a much longer time is a key advantage of empirical force field simulations, reducing the noise enough to resolve accurate values of derivative quantities like γ in single simulations, whereas *ab initio* approaches generally obtain γ only by fitting a functional form to a series of simulations (the result therefore depending on the form of the adopted function). On the other hand, all empirical MD calculations are limited by the accuracy of the assumed force field. In this study, we pursued a combined approach by tuning a force field using a small set of *ab initio* simulations and then defining the systematic behavior of γ with a large campaign of empirical MD runs using the optimized force field.

2. METHODS

Molecular dynamics is a semi-classical approach to simulating material behavior that uses Newton's laws of motion to track the trajectories of atoms, treated as classical particles moving under the influence of certain forces. In empirical potential molecular dynamics (EPMD), a predefined functional form and set of parameters are used to describe the potential energy resulting from interactions among the atoms. Given the initial positions and velocities of all the atoms, their positions and velocities at each following timestep can be calculated. By analyzing the energies, trajectories and positions of the atoms at each timestep or averaged over time, one can calculate first-order macroscopic properties such as density, pressure, temperature, internal energy, and enthalpy; transport properties such as viscosity and diffusion coefficients; derivative thermodynamic properties such as heat capacity, thermal expansion coefficient, and γ; and microscopic structural properties such as radial distribution functions, atomic coordination numbers, bond lifetimes, etc.

In this study, we designed a simulation campaign around determining with optimum accuracy and precision

the γ of the composition that appears at the 1 atm eutectic point in the binary system anorthite-diopside. This is a mixture of 36 mol% anorthite component ($CaAl_2Si_2O_8$) and 64 mol% diopside component ($CaMgSi_2O_6$). The minimum exact representation of this composition is 9 formula units of $CaAl_2Si_2O_8$ plus 16 formula units of $CaMgSi_2O_6$, which is 277 total atoms (25 Ca, 16 Mg, 18 Al, 50 Si, 168 O). This 277-atom system was used for our *ab initio* molecular dynamics (AIMD) simulations. For EPMD simulations, we multiplied the number of atoms of each element by four to obtain a system of 1108 atoms. Various periodic systems containing 277, 554 and 1108 atoms were tested, and the conclusions are unaffected, although the results from the smaller systems have more noise and it becomes more difficult to discern patterns in the values of γ.

AIMD simulations were conducted with the Vienna *ab initio* Simulation Package (VASP) (Kresse and Furthmüller, 1996) using Projector-Augmented Wave (PAW) representations of the core electrons (Blöchl, 1994), PBE-D3 cross-correlation functional (Grimme et al., 2010; Grimme et al., 2011), a plane-wave basis with an energy cutoff of 520 eV, and sampling of the Brillouin zone at the Γ-point only. The electronic occupations were populated according to the Mermin finite temperature formulation of DFT (Mermin, 1965). These computational parameter choices are similar to standard methods that have been applied to silicate melts by other groups (Karki et al., 2011). The time step is 1 fs. We conducted *N-V-T* simulations in a cubic box with periodic boundary conditions and a Nosé-Hoover thermostat. Volume was adjusted to reach pressures of approximately 0, 4 and 50 GPa at 1673 K. Then temperature was increased to 4500 K at a rate of 100 K/ps to find the internal energy as a function of temperature. Next, the system was equilibrated using an *N-V-E* ensemble at the energies corresponding to 2000, 2500, 4000, and 4500 K for 3 ps each. For each pair of states 500 K apart, the average pressure, average isochoric heat capacity $C_V = \left(\frac{\Delta E}{\Delta T}\right)_V$, and average $\gamma = V\left(\frac{\Delta P}{\Delta E}\right)_V$ were obtained by finite difference and stored for subsequent tuning of the empirical force field.

The EPMD simulations, following Spera et al. (2009), were based on the transferrable pairwise potential developed by Matsui (1998), which combines a van der Waals interaction, expressed by an exponential repulsive term and an r^{-6} attractive term, and a Coulomb interaction with fractional atomic charges. However, Ghiorso et al. (2009) showed that this potential, as calibrated by Matsui, is only accurate for anorthite liquid up to about 25 GPa pressure. Hence, we sought to adjust the parameters of this force field to obtain a better broad range fit to our AIMD results at all the pressures of interest.

To improve the original Matsui force field to match *ab initio* results, we did not modify the fractional charges on each ion; we only modified the parameters of the van der Waals interactions. The parameters governing each atom pair were transformed to yield three parameters (see Supplementary material), effectively the equilibrium separation distance r_0, the depth of the potential well D_0, and the curvature of the potential at the minimum ζ.

Atom pair interactions were grouped into cation-oxygen, oxygen–oxygen, and cation-cation interactions. As cation-cation interactions are weak in silicate liquids, we focused on the cation-oxygen and oxygen–oxygen pairs. To reduce the dimensionality of the optimization, all cation-oxygen pairs were grouped together and subjected to the same rescaling. That leaves six free parameters in the rescaling (i.e., multipliers for D_0, r_0, and ζ for all cation-oxygen pairs and for oxygen–oxygen pairs). An objective function (see Supplementary material) was designed with a weighting of the misfits to four pressure values, two C_V values, and two γ values from the AIMD simulations. This objective function was minimized with both the BFGS search algorithm (Broyden, 1970; Fletcher, 1970; Goldfarb, 1970; Shanno, 1970) and the gradient descent algorithm. The resulting optimized force field was then used in all subsequent EPMD simulations; the parameters, transformed back to the original form necessary to encode the force field in LAMMPS simulations, are given in the Supplementary material.

Armed with this optimized potential, we conducted EPMD simulations using LAMMPS (Plimpton, 1995) in the range of 1500 K to 6500 K and 0 GPa to 150 GPa. *N-V-T* simulations used a Nosé-Hoover thermostat. We also explored *N-P-T* simulations with a barostat in order to compute the alternative thermal volume parameter $R = P\left(\frac{\partial V}{\partial H}\right)_P$ for comparison in functional dependence and simplicity of use to γ. The LAMMPS simulation box was first compressed (or expanded) in volume to achieve pressures from 1 atm to 150 GPa at 6500 K. Next, each isochore was calculated by cooling to the target temperature series using *N-V-T* (for γ) or *N-P-T* (for R) ensembles. Cooling rates ranging from 0.005 to 1 ns per temperature interval were tested and the conclusions are unaffected. γ was calculated by transferring snapshots of atomic positions and velocities taken every 500 K from the N-V-T runs to 500 ps *N-V-E* runs at different states and then applying a finite difference calculation based on the averaged pressure and internal energy of the last 200 ps. Likewise R was calculated by transferring snapshots of *N-P-T* runs to 200 ps *N-P-H* simulations. The so-called thermal pressure coefficient $\left(\frac{\partial P}{\partial T}\right)_V$ was also obtained from the *N-V-T* calculations.

3. RESULTS

3.1. General behavior of γ

EPMD simulations were conducted along 12 isochores, corresponding to a pressure range at 2000 K from 1 atm to 150 GPa, at internal energies corresponding to temperatures from 1500 K to 6500 K. Volumes are expressed relative to V_a, the volume of the simulation that yields 1 atm pressure at 2000 K. The lowest-temperature, lowest-volume simulations showed signs of glassy rather than liquid behavior, based on their heat capacities and atomic trajectories. These yielded anomalous values of γ and were excluded from subsequent analysis. The remaining data, viewed as γ vs. E with points at equal volume shown in a common color, are plotted in Fig. 1. It is clear immediately that the general behavior of γ vs. V expected from previous

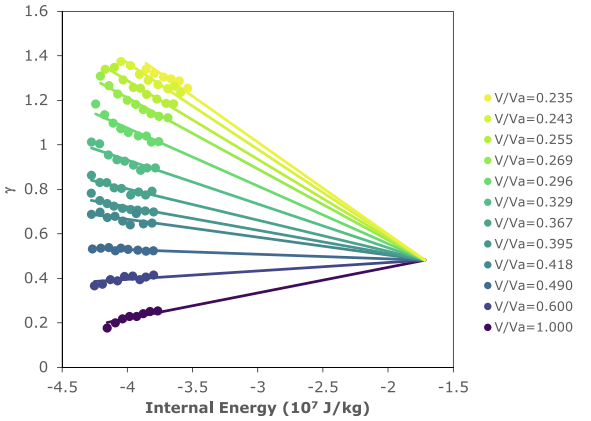

Fig. 1. Values of the Grüneisen parameter, γ, determined by finite difference from consecutive N-V-E state points in empirical molecular dynamics simulations, plotted against internal energy and colored by volume relative to the volume (V_a) that yields 1 atm pressure at 2000 K. The lines are a series linear regressions to each set of isochoric values, forced to intersect at a common point.

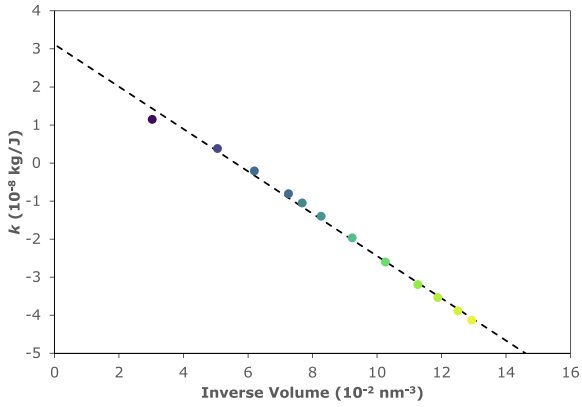

Fig. 2. The slopes k of the isochores in γ vs. E space are plotted against the reciprocal of volume. Dots show the individual fits to each isochore plotted in Fig. 1. The dashed line shows a linear regression expressing a systematic dependence of slope on $1/V$.

simulation and experimental campaigns is present: γ is a strong function of V, monotonically increasing with decreasing volume at any constant value of E. Moreover, the Mie-Grüneisen approximation is a reasonable first-order description of the results: the dependence on volume, across the studied range, is the main source of variation in γ (e.g., a range from 0.25 to 1.35 between $V/V_a = 1.000$ and 0.243 at $E = -4.0 \times 10^7$ J/kg), whereas the dependence on E at constant V is comparatively small (a maximum range of about 0.2 from 1500 K to 6500 K, for example at $V/V_a = 0.296$). Nevertheless, the variations of γ as a function of E at constant V are well-resolved, real, and systematic. No Mie-Grüneisen model can fit these data to better than $\pm 20\%$ accuracy. At large volume (low pressure), γ systematically increases with increasing E at constant V. This positive dependence decreases with decreasing volume until, at a particular intermediate volume (or pressure), γ is nearly independent of E. Then a negative dependence develops, increasing with decreasing volume to become a significant trend of decreasing γ with increasing E at small values of V (or high P).

Noting that each isochore in γ vs. E is approximately linear and that these lines converge at high E towards a common point, we fitted a line to each isochore in the data, as shown in Fig. 1. In this fitting exercise, the slope of each isochore is fit independently, although all are forced to intersect at a common point. The slopes (k) of these fit lines are plotted against the inverse of volume in Fig. 2. Here we see that the slopes of the $\gamma - E$ isochores themselves are approximately a linear function of inverse volume. A linear fit to k vs. $1/V$ yields $R^2 = 0.996$.

3.2. The gamma model

The observations that (1) the variation in γ with E at constant V is nearly linear along each isochore (Fig. 1), that these isochores converge to a common point (also Fig. 1), and that the slopes of these lines are very nearly a linear function of inverse volume (Fig. 2) together motivate the introduction of a simple, four-parameter model for fitting all these data as a function $\gamma(E, V)$. The model is expressed by two equations:

$$\gamma = k(E - E^*) + \gamma^* \tag{1}$$

$$k = \frac{a}{V} + b \tag{2}$$

where a, b, E^*, and γ^* are the four parameters of the model. In a plot of γ vs. E, the isochores all intersect at the reference point (E^*, γ^*). We note that this reference point plots at very high energy, far beyond the stability field of the liquid phase, and we do not consider it to have any physical significance; it is merely a convenience to simplify the model form. The slopes k of the various isochores are a linear function of the inverse volume, with slope a and intercept at infinite volume b. The best fitting model is shown in Fig. 3 (which differs from Fig. 1 in that the slopes of all the lines are governed in Fig. 3 by the four-parameter

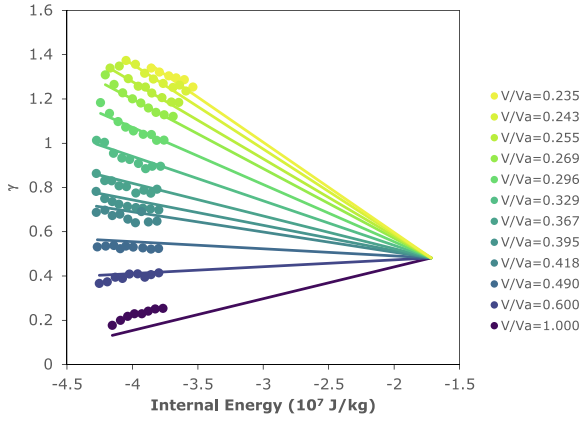

Fig. 3. The values of γ vs. E along isochores, repeated from Fig. 1, are now compared to the best-fitting four-parameter model, in which the lines representing each isochore are required to intersect at a common point and also to follow a systematic linear dependence of their slope on $1/V$.

model, whereas in Fig. 1 each line is an independent regression for the slope of a particular isochore). This model leaves a residual variance of 0.66% of the variance of the complete set of liquid-like calculated values of γ.

By comparison, any Mie-Grüneisen type model is likely to require at least three parameters (e.g., $(\gamma/\gamma_0) = (V/V_0)^q$ has three parameters, γ_0, V_0, and q) and for our data set the residual variance of a Mie-Grüneisen model can be no less than 1.24% of the original variance, given the clear E dependence of the data (in fact this particular three-parameter form has residual variance of 2.02%). Thus the one extra parameter offers at least a factor of two reduction in total misfit relative to any Mie-Grüneisen model and a factor of three relative to the q power-law form.

4. DISCUSSION

4.1. Comparison with other models

4.1.1. Fitting EPMD data to Birch-Murnaghan equation of state plus thermal pressure

The Birch-Murnaghan equation of state describes the relationship between volume and pressure using finite elastic strain (Birch, 1947). This model is used to derive the isentrope upon compression and a thermal pressure term is required to account for the temperature dependence. The thermal pressure described in the original Mie-Grüneisen model does not contain temperature dependence and thus has limitations in the fitting of Hugoniot data as shown below. Although the main intent of the simulation campaign is to motivate the design of a model form that can be fit to experimental data, we fitted the thermal equations of state resulting from combining a Birch-Murnaghan isentrope with either a Mie-Grüneisen or a $\gamma(E, V)$ model to the *P-V-E* dataset from the EPMD simulations. The results and fitted parameters are given in the Supplementary material. The $\gamma(E, V)$ model is a slightly better fit (RMS error in pressure is 0.15 GPa vs. 0.17 GPa for the Mie-Grüneisen model). This difference is modest, because both functional forms can interpolate well among densely sampled simulation data. The power of the new model arises when large extrapolations in energy space are required and when data are sparse, as is typically the case with experimental shock wave data.

4.1.2. Mie-Grüneisen fits to experiments

Within the overall category of Mie-Grüneisen models that force γ to be a one-parameter function $\gamma(V)$, a variety of functional forms have been proposed and several are in common use (Shanker et al., 2007; Peng et al., 2007). Some of these were selected for convenience or to minimize the number of free parameters, while others were designed to explicitly incorporate physical constraints or limiting values such as the Thomas–Fermi limit, usually interpreted to require $\gamma = 2/3$ at zero volume. However, in the shock wave literature the most widely used form is the q-model, $(\gamma/\gamma_0) = (V/V_0)^q$. For solids, q is positive and often close to unity; in fact, the simplest model of a volume-dependent Grüneisen parameter assumes $q = 1$, i.e. constant γ/V. For liquids, however, where it is now widely acknowledged that γ increases as volume decreases, this functional form requires $q < 0$. In fact, fits to a variety of silicate liquid compositions where γ_0 is known and sparse high-pressure constraints are available from shock wave data all yield $q = -1.5 \pm 0.5$ (Asimow, 2018). The challenge with values of $q < -1$ is that this form is concave-up on plots of γ vs. V and diverges to large positive values of γ as V approaches zero. Fits to data extending up to about 150 GPa with this form already begin to predict excessive thermal pressure terms at compression only modestly exceeding the calibrated range. Thus, for example, the $\gamma(V)$ function proposed for forsterite (Mg_2SiO_4) liquid by Thomas and Asimow (2013), with $q = -1.51$, fits experimental data of Mosenfelder et al. (2007) and simulation data of de Koker et al. (2008), both extending to 200 GPa and $V/V_0 = 0.5$. However, it cannot fit the recent very high-pressure data of Davies et al. (2020), which show that γ stops increasing along the principal Hugoniot of forsterite at $V/V_0 = 0.5$ and begins to decrease towards the Thomas–Fermi limit beyond this range. Since the shallow-release experiments of Davies et al. (2020) constrain γ for forsterite liquid only close to the Hugoniot (a one-parameter path through *P-V-E* space), it is not clear how much of this decrease is due to decreasing volume and how much might be due to increasing internal energy. Davies et al. (2020) propose a six-parameter function to fit their data as a function of volume only.

4.1.3. Previous empirical molecular dynamics studies

There are two previous simulation-based studies that have developed functional forms for the equation of state and thermodynamic properties of anorthite liquid under significant compression; one uses EPMD and the other AIMD.

The EPMD simulation data of Spera et al. (2009), using the Matsui potential and covering 3500–6100 K and 0.84–120 GPa, were fit to two complex models by Ghiorso et al. (2009). Both models required segmentation into separate low-pressure and high-pressure fits and each has many parameters that make them unsuitable for fitting to sparse experimental data. Notably, of the models proposed by Ghiorso et al. (2009), neither the high-pressure segment of the fit to the Ghiorso (2004) model nor the Rosenfeld-Tarazona model are consistent with the Mie-Grüneisen approximation, as can be seen by the spreading of isotherms on the γ vs. P plots in that work. Here, for purposes of comparison, we have replotted the low-pressure segment of the Rosenfeld-Tarazona model of Ghiorso et al. (2009) as isochores in γ vs. E space (Fig. 4a). It is evident that the general form of this portion of the equation of state of anorthite liquid proposed by Ghiorso et al. (2009) shares the features we have identified in our simulation data for diopside-anorthite liquid: γ increases strongly with decreasing V, depends significantly on E, is approximately a linear function of E at each constant V, and transitions from a positive slope at large V to a negative slope at small V. Although the original simulations of Spera et al. (2009) were not optimized for obtaining high-precision estimates of γ, both the raw data at relatively low pressure and the model adopted for fitting those low-pressure data could

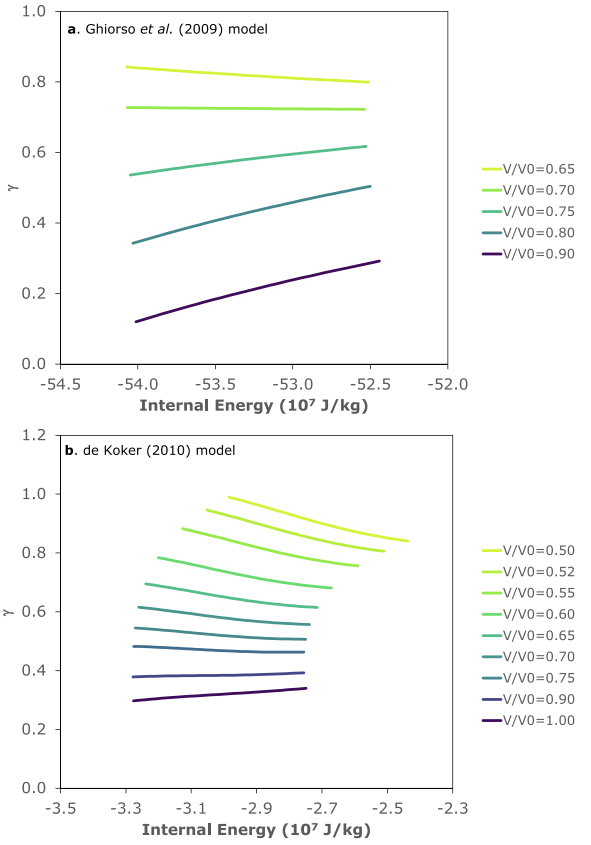

Fig. 4. Comparison of two published γ models. (a) The $\gamma(V,E)$ relationship predicted by the low-pressure segment of the Rosenfeld-Tarazona model of Ghiorso et al. (2009). (b) The $\gamma(V,E)$ relationship predicted by the Helmholtz free energy parameterization of De Koker (2010).

readily be fit with good accuracy by the model form of Eqs. 1 and 2 of this work. Given the weakness of the original Matsui potential at higher pressures, pointed out by Spera et al. (2009), the low-pressure segment of the data makes the most relevant point of comparison. We conclude that our proposed systematic behavior and simple functional form for $\gamma(E,V)$ are consistent with the EPMD simulation results on anorthite.

4.1.4. Previous ab initio molecular dynamics studies

AIMD on viscous liquid silicate systems requiring large numbers of atoms and long integration times are computationally challenging. Only a few groups have published such studies, including only one study of anorthite (and none on CaO-MgO-Al_2O_3-SiO_2 liquids such as that studied herein). They are limited to fairly high temperatures (>3000 K) by the computational constraints and the need to obtain ergodicity in the simulation. Direct determination of γ and other second-order quantities from finite differences between adjacent state points yields low precision due to the inherent uncertainty in pressure and energy at each state point in an N-V-T simulation campaign. Hence, De Koker (2010) adopted the approach of using the simulation results first to fit a functional form to the equation of state, namely the Helmholtz free energy model of De Koker and Stixrude (2009), and then deriving γ by differentiation of the fitted model. Although De Koker (2010) emphasized only the volume dependence of the resulting values of γ, in fact this model also yields an internal energy dependence quite similar to that of the EPMD study of Ghiorso et al. (2009), with nearly linear isochores, positive slopes at high volume, and negative slopes at low volume (Fig. 4b). These results too are readily fitted to our proposed four-parameter functional form, which is again much simpler to apply than the fundamental relation of De Koker and Stixrude (2009).

4.1.5. Enthalpy formulation and the R parameter

Nagayama (2016) and Nagayama (2017) discussed the shortcomings of the Mie-Grüneisen model for fitting the high-temperature equation of state of liquid metals obtained from shock Hugoniot data on porous starting materials. Those works suggested the use of an enthalpy formulation or Rice-Walsh equation of state, in which the Wu-Jing or R parameter takes the place of γ. In liquid metals, Nagayama (2016) found that γ is not a one-parameter function of volume, but that R is, in fact, a one-parameter function of P with a simple, universal form applicable to all the metals considered. This result motivated us to examine the systematics of R in our simulations. We did not find such a simple behavior in liquid silicates. R is a function of both P and H and offered no obvious advantage in simplicity over γ. Hence we focused our effort on extending the internal energy formulation with thermal pressure and do not recommend an enthalpy formulation with a thermal volume term for use in silicate liquids.

We also considered whether the thermal pressure coefficient $\left(\frac{\partial P}{\partial T}\right)_V$ can be treated as a function only of volume. At small volumes (high pressures), it depends significantly on T, and offers no advantage over γ in this regard. See the supplementary information.

4.2. Application: fitting to experimental results

A number of constraints on the thermal EOS of the studied anorthite-diopside eutectic liquid composition are available as a result of a series of shock compression studies. Rigden et al. (1984) and Rigden et al. (1988) pioneered the method of shock travel time measurements in encapsulated, pre-heated silicate liquids and published eight shock velocity measurements defining the Hugoniot of anorthite-diopside liquid from an initial super-liquidus condition of 1673 K, extending up to 34 GPa. Asimow and Ahrens (2010) published four additional state points on the same pre-heated liquid Hugoniot, reaching 125 GPa. Asimow and Ahrens (2010) also published a single shock travel time data point obtained from a room-temperature aggregate of solid anorthite and diopside that underwent shock melting and achieved a pressure of 133 GPa. Finally, Asimow et al. (2018) used the rarefaction overtake technique to obtain a measurement of the sound speed in anorthite-diopside liquid shocked to 132 GPa.

The 13 shock travel time measurements on anorthite-diopside liquid at 1673 K, together with known properties of the projectile and capsule materials and an estimate of

the initial liquid density (Ai and Lange, 2008), define a linear Hugoniot in shock velocity (U_S) vs. particle velocity (u_p). Knowing the initial E difference between 1673 K liquid and 300 K solid aggregate from thermochemical data and assuming γ is only a function of V, it is therefore possible to precisely fit the offset of the single shock state derived from initially 300 K solid from the pre-heated liquid Hugoniot in U_S-u_p space by choosing a value of γ at the volume of that shock state. Indeed, the resulting $\gamma/\gamma_0 = 3.07$, at $(V/V_0) = 0.503$, implies $q = -1.63$ (Asimow and Ahrens, 2010). However, this approach provides no information on any possible E dependence of γ, since there is only one constraint.

On the other hand, each of the $U_S - u_p$ data points can be transformed using the Rankine-Hugoniot jump conditions into a $P - V - E$ state point. When the 12 resulting data points on the pre-heated liquid Hugoniot are fitted to an equation of state, in this case a 3rd-order Birch-Murnaghan isentrope plus a Mie-Grüneisen thermal pressure term (assuming the q-form for the volume dependence of γ), the shape of the pre-heated liquid Hugoniot data themselves already constrain the γ function. Hence it is not necessarily possible to simultaneously fit both the 12 pre-heated liquid Hugoniot points and the single shock state point obtained by shocking the 300 K solid aggregate. In fact, the best fit model given by Asimow and Ahrens (2010) misses this data point by 2.8σ in P-V space (Fig. 5, orange dashed curve). In other words, in a Mie-Grüneisen context (or at least with the specific q-form for the volume dependence of γ), the combined data set appears to be inconsistent. Essentially, the rapid increase in γ needed to match the divergence of the pre-heated liquid Hugoniot from the isentrope during the initial rapid decrease in volume at low pressure yields a value of γ at $(V/V_0) = 0.503$ that is much too large to fit the relatively small pressure difference between the pre-heated liquid Hugoniot and the point obtained by shocking 300 K solid aggregate, again in the context of the simple $\gamma(V)$ model previously assumed (see Table 2).

Table 1
Fitting parameters for EPMD results in Fig. 3 using the $\gamma(V,E)$ model.

Parameters	Values
γ^*	0.481
E^* (J/kg)	-1.717×10^7
a (nm^3 kg/J)	-5.3329×10^{-7}
b (kg/J)	3.1206×10^{-8}

V in this fit is the absolute volume of the 1108 atom simulations, in nm^3.

In this context, the introduction of the new $\gamma(V,E)$ model developed in this work is quite promising. It allows for the rapid increase in E during strong shock compression to compensate for the decrease in V and yield a γ function that may be able to fit all the constraints. In fact, there is an additional experimental constraint that was not available to Asimow and Ahrens (2010), namely the sound speed measurement. As shown, e.g., by Brown and McQueen (1986), a sound speed measurement at a point along a known liquid Hugoniot gives a local measure of γ that does not depend on a Mie-Grüneisen assumption. Hence, we fitted the combined shock velocity and sound speed data set for anorthite-diopside liquid to a 3rd order Birch-Murnaghan isentrope plus our new four-parameter $\gamma(V,E)$ model. Ambient pressure constraints on K_{S0} and γ_0 from density and ultrasonic data (Ai and Lange, 2008)

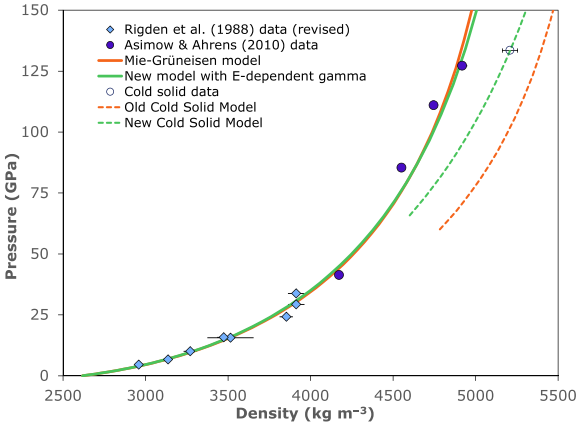

Fig. 5. Equation of state fitting to shock wave data on anorthite-diopside liquid. The orange curves show a 3rd order Birch-Murnaghan isentrope plus Mie-Grüneisen thermal pressure model whereas the green curves show a model adopting the $\gamma(E,V)$ model developed in this work. In both cases, the filled symbols and solid curves show the pre-heated liquid Hugoniot and the open symbol and dashed curves show the shock states obtained by shock melting an isochemical cold solid aggregate. All the equations necessary to plot these data and model fits are provided in the supplementary information.

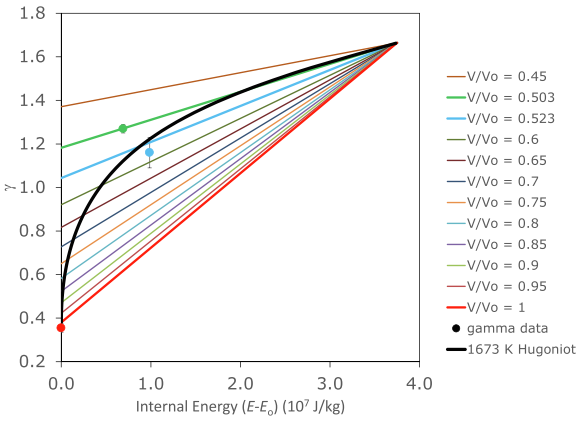

Fig. 6. The fitted $\gamma(E,V)$ model compared to direct experimental constraints on γ. The black curve is the trace of the pre-heated liquid Hugoniot. The red symbol is γ_0 based on 1 atm data, compared to the red V/V_0 isochore. The green symbol is the constraint from the cold solid aggregate experiment, compared to the green $V/V_0 = 0.503$ isochore. The cyan symbol is the constraint from the sound speed measurement, compared to the cyan $V/V_0 = 0.522$ isochore. (For interpretation of the references to colour in this figure legend, the reader is referred to the web version of this article.)

were imposed as well. This model (Fig. 5, green curves) is able to fit all the data within their uncertainty. The particular $\gamma(V,E)$ model with the best-fitting parameters is compared to the direct constraints on γ from ambient pressure data, the cold solid Hugoniot point, and the sound speed datum in Fig. 6. The parameters are given in Table 2 alongside the parameters of the original fit.

The Grüneisen parameter, by definition, parameterizes the thermal pressure of an equation of state, allowing calculation of states offset in internal energy from a reference state at equal volume. However, by thermodynamic identities, γ also defines the isentropic gradient in temperature-volume space: $\gamma = -\left(\frac{\partial lnT}{\partial lnV}\right)_S$. Rapidly convecting systems such as deep molten layers created in early planetary evolution by dissipation of kinetic energy from giant impacts evolve to an approximately isentropic temperature profile. Therefore, an important geophysical application of a model for γ of silicate liquids is the calculation of isentropes in planetary magma oceans. Although diopside-anorthite eutectic is not a plausible composition for a molten terrestrial mantle, comparison of the isentropes computed for a Mie-Grüneisen model and for the $\gamma(V,E)$ model of this composition illustrate the magnitude of the difference that is expected for a bulk silicate Earth composition. Fig. 7 shows three pairs of isentropes, with equal foot temperatures of 1673 K, 2273 K, and 2873 K, using the $\gamma(V)$ model of Asimow and Ahrens (2010) and the $\gamma(V,E)$ model fitted in this work. The isentropes for the $\gamma(V,E)$ model are, at each foot temperature, more strongly concave down, due to the decrease in the rate of increase in γ as E increases along the isentrope. The differences in slope grow larger for isentropes with hotter foot temperatures, because they access higher energy states where the energy dependence becomes more significant. For temperatures most relevant to superliquidus magma oceans, the difference between the two models in temperatures near the core-mantle boundary for isentropes with equal foot temperature grows to > 500 K. Computed isentropes can be compared to experimentally defined (Fiquet et al., 2010; Andrault et al., 2011) or computed (Boukaré et al., 2015) liquidus curves to estimate the potential temperature of incipient crystallization and the depth where crystallization is expected to begin. The more concave-down shape of the isentropes computed with the $\gamma(V,E)$ model increase the range of liquidus shapes and slopes that lead to initial crystallization at the bottom of the mantle and make it less likely that crystallization began in the middle of the magma ocean.

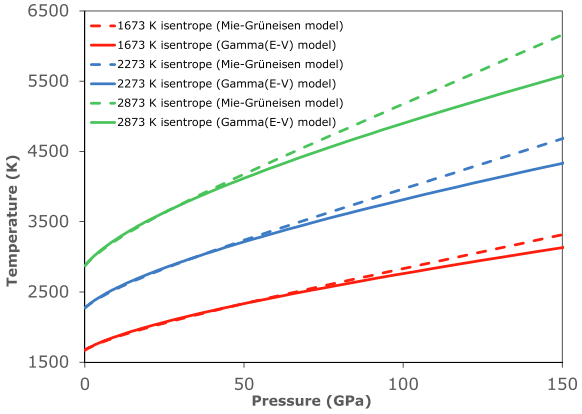

Fig. 7. Comparison of *T*-*P* shapes of liquid isentropes with foot temperatures of 1673, 2273, and 2873 K computed with the thermal Mie-Grüneisen equation of state of Asimow and Ahrens (2010) (dashed curves) and with the $\gamma(V,E)$ model of the present work. (solid curves).

5. CONCLUSIONS

We designed a set of empirical potential molecular dynamics calculations around accurate calculation of the Grüneisen parameter of a silicate liquid composition. The force field was tuned to a select set of *ab initio* molecular dynamic simulations to improve its portability across the pressure range of interest for the terrestrial mantle. In agreement with earlier simulation studies that show E-dependent behavior of γ in silicate and simple liquids, we find a systematic behavior of volume and energy-dependent variations in γ. Although sophisticated, parameter-rich functional forms are needed to fit all the thermodynamic properties of silicate liquids or to extrapolate to extreme conditions, we introduce a simplified model with only a few parameters that fits the simulation results well. Applying this model form to experimental shock wave data on the same liquid composition used in the calculations yields excellent results and a more predictive, wide-ranging, and powerful fit to the variety of data types available. Extension of this concept to other silicate and oxide

Table 2
Comparison of the original Mie-Grüneisen fit and the $\gamma(V,E)$ model fit.

Parameters	Original Mie-Grüneisen fit	New fit
V_0 (m^3/kg)	0.0003829 ± 0.0001	0.0003829 ± 0.0001
K_{S0} (GPa)	22.98 ± 0.30	22.93 ± 0.21
K'_S	5.36 ± 0.43	5.59 ± 0.11
Model specific Parameters	$\gamma_0 = 0.356$ (at V_0; fixed) $q = -2.06 \pm 0.54$	$\gamma^* = 1.663 \pm 0.01$ $E^* = (3.75 \pm 0.07) \times 10^7$ J/kg $a = (-8.26 \pm 0.05) \times 10^{-12}$ m^3/J $b = (5.59 \pm 0.02) \times 10^{-8}$ kg/J ($\gamma_0 = 0.380$ at V_0, E_0)

liquid compositions will enable improved modeling of the evolution of early terrestrial magma oceans.

6. RESEARCH DATA

Research Data associated with this article (the V-P-E simulation points shown in Figs. 1 and 3) can be accessed at the CaltechDATA repository at https://doi.org/10.22002/D1.1921.

Declaration of Competing Interest

The authors declare that they have no known competing financial interests or personal relationships that could have appeared to influence the work reported in this paper.

ACKNOWLEDGMENTS

This work is funded by the Office of Naval Research, award numbers N00014-20–1-2603 (to PDA) and N00014-19–1-2081 (to WAG), and by the National Science Foundation, award number 1725349. The computations presented here were conducted in the Resnick High Performance Center, a facility supported by Resnick Sustainability Institute at the California Institute of Technology.

APPENDIX A. SUPPLEMENTARY MATERIAL

Supplementary data associated with this article can be found, in the online version, at https://doi.org/10.1016/j.gca.2021.10.005.

REFERENCES

Ai Y. and Lange R. A. (2008) New acoustic velocity measurements on CaO-MgO-Al_2O_3-SiO_2 liquids: Reevaluation of the volume and compressibility of $CaMgSi_2O_6$-$CaAl_2Si_2O_8$ liquids to 25 GPa. *J. Geophys. Res. B: Solid Earth* **113**, B04203.

Andrault D., Bolfan-Casanova N., Nigro G. L., Bouhifd M. A., Garbarino G. and Mezouar M. (2011) Solidus and liquidus profiles of chondritic mantle: Implication for melting of the earth across its history. *Earth Planet. Sci. Lett.* **304**, 251–259.

Arp V., Persichetti J. and Chen G. b. (1984) The Grüneisen parameter in fluids. *J. Fluid Eng.* **106**, 193–200.

Asimow P. D. (2018) Melts under extreme conditions from shock experiments. In *Magmas Under Pressure*. Elsevier, pp. 387–418.

Asimow P. D. and Ahrens T. J. (2010) Shock compression of liquid silicates to 125 GPa: The anorthite-diopside join. *J. Geophys. Res. B: Solid Earth*, 115.

Asimow, P. D., Pardo, O. S., Hu, J. (2018). Sound speed and temperature in shock-compressed silicate liquids: Direct constraints on Grüneisen parameters and heat capacities, in: AGU Fall Meeting Abstr., pp. MR31A–06.

Bertoldi D. S., Miranda E. N. and Guillermet A. F. (2014) Revisiting the thermostatistics of the Grüneisen parameters and applications to quasiharmonic solids. *J. Phys. Chem. Solids* **75**, 1147–1151.

Birch F. (1947) Finite elastic strain of cubic crystals. *Phys. Rev.* **71**, 809–824.

Blöchl P. E. (1994) Projector augmented-wave method. *Phys. Rev. B* **50**, 17953.

Boehler R. and Ramakrishnan J. (1980) Experimental results on the pressure dependence of the Grüneisen parameter: A review. *J. Geophys. Res. B: Solid Earth* **85**, 6996–7002.

Boukaré C. E., Ricard Y. and Fiquet G. (2015) Thermodynamics of the MgO-FeO-SiO_2 system up to 140 GPa: Application to the crystallization of earth's magma ocean. *J. Geophys. Res. B: Solid Earth* **120**, 6085–6101.

Boyet M., Blichert-Toft J., Rosing M., Storey M., Télouk P. and Albarède F. (2003) ^{142}Nd evidence for early earth differentiation. *Earth Planet. Sci. Lett.* **214**, 427–442.

Brown J. M., Furnish M. D. and Mcqueen R. G. (1987) Thermodynamics for (Mg, Fe)$_2SiO_4$ from the Hugoniot. *High-Press. Res. Miner. Phys.*, 373–384.

Brown J. M. and McQueen R. G. (1986) Phase transitions, Grüneisen parameter, and elasticity for shocked iron between 77 GPa and 400 GPa. *J. Geophys. Res. B: Solid Earth* **91**, 7485–7494.

Broyden C. G. (1970) The convergence of a class of double-rank minimization algorithms 1. general considerations. *IMA J. Appl. Math.* **6**, 76–90.

Davies E. J., Carter P. J., Root S., Kraus R. G., Spaulding D. K., T S. S. and B J. S. (2020) Silicate melting and vaporization during rocky planet formation. *J. Geophys. Res. E: Planets* **125**, e2019JE006227.

De Koker N. (2010) Structure, thermodynamics, and diffusion in $CaAl_2Si_2O_8$ liquid from first-principles molecular dynamics. *Geochim. Cosmochim. Acta* **74**, 5657–5671.

De Koker N. and Stixrude L. (2009) Self-consistent thermodynamic description of silicate liquids, with application to shock melting of MgO periclase and $MgSiO_3$ perovskite. *Geophys. J. Int.* **178**, 162–179.

Fiquet G., Auzende A., Siebert J., Corgne A., Bureau H., Ozawa H. and Garbarino G. (2010) Melting of peridotite to 140 gigapascals. *Science* **329**, 1516–1518.

Fletcher R. (1970) A new approach to variable metric algorithms. *Comput. J.* **13**, 317–322.

Ghiorso M. S. (2004) An equation of state for silicate melts. i. formulation of a general model. *Am. J. Sci.* **304**, 637–678.

Ghiorso M. S., Nevins D., Cutler I. and Spera F. J. (2009) Molecular dynamics studies of $CaAl_2Si_2O_8$ liquid. part II: Equation of state and a thermodynamic model. *Geochim. Cosmochim. Acta* **73**, 6937–6951.

Goldfarb D. (1970) A family of variable-metric methods derived by variational means. *Math. Comput.* **24**, 23–26.

Grimme S., Antony J., Ehrlich S. and Krieg H. (2010) A consistent and accurate ab initio parametrization of density functional dispersion correction (dft-d) for the 94 elements h-pu. *J. Chem. Phys.* **132**, 154104.

Grimme S., Ehrlich S. and Goerigk L. (2011) Effect of the damping function in dispersion corrected density functional theory. *J. Comput. Chem.* **32**, 1456–1465.

Grüneisen E. (1912) Theorie des festen zustandes einatomiger elemente. *Ann. Phys.* **344**, 257–306.

Halliday A., Wänke H., Birck J. L. and Clayton R. (2001) The accretion, composition and early differentiation of Mars. *Space Sci. Rev.* **96**, 197–230.

Hofmann A. W. (1988) Chemical differentiation of the earth: the relationship between mantle, continental crust, and oceanic crust. *Earth Planet. Sci. Lett.* **90**, 297–314.

Holzapfel W. B. (2005) Progress in the realization of a practical pressure scale for the range 1–300 GPa. *High Pressure Res.* **25**, 87–99.

Jing Z. and Karato S. i. (2011) A new approach to the equation of state of silicate melts: An application of the theory of hard sphere mixtures. *Geochim. Cosmochim. Acta* **75**, 6780–6802.

Karki B. B., Bohara B. and Stixrude L. (2011) First-principles study of diffusion and viscosity of anorthite ($CaAl_2Si_2O_8$) liquid at high pressure. *Am. Mineral.* **96**, 744–751.

Knopoff L. and Shapiro J. (1970) Pseudo-Grüneisen parameter for liquids. *Phys. Rev. B* **1**, 3893.

de Koker N. P., Stixrude L. and Karki B. B. (2008) Thermodynamics, structure, dynamics, and freezing of Mg_2SiO_4 liquid at high pressure. *Geochim. Cosmochim. Acta* **72**, 1427–1441.

Kresse G. and Furthmüller J. (1996) Efficiency of ab-initio total energy calculations for metals and semiconductors using a plane-wave basis set. *Comput. Mater. Sci.* **6**, 15–50.

Labrosse S., Hernlund J. and Coltice N. (2007) A crystallizing dense magma ocean at the base of the earth's mantle. *Nature* **450**, 866–869.

Matsui M. (1998) Computational modeling of crystals and liquids in the system Na_2O-CaO-MgO-Al_2O_3-SiO_2. *Geophys. Monogr. Ser.* **101**, 145–151.

Mausbach P., Köster A., Rutkai G., Thol M. and Vrabec J. (2016) Comparative study of the Grüneisen parameter for 28 pure fluids. *J. Chem. Phys.* **144**, 244505.

Mermin N. D. (1965) Thermal properties of the inhomogeneous electron gas. *Phys. Rev.* **137**, A1441.

Mie G. (1903) Zur kinetischen theorie der einatomigen körper. *Ann. Phys.* **316**, 657–697.

Mosenfelder J. L., Asimow P. D. and Ahrens T. J. (2007) Thermodynamic properties of Mg_2SiO_4 liquid at ultra-high pressures from shock measurements to 200 GPa on forsterite and wadsleyite. *J. Geophys. Res. B: Solid Earth*, 112.

Mosenfelder J. L., Asimow P. D., Frost D. J., Rubie D. C. and Ahrens T. J. (2009) The $MgSiO_3$ system at high pressure: Thermodynamic properties of perovskite, postperovskite, and melt from global inversion of shock and static compression data. *J. Geophys. Res. B: Solid Earth*, 114.

Nagayama K. (2016) Formulation of the rice-walsh equation of state based on shock hugoniot data for porous metals. *J. Appl. Phys.* **119**, 195901.

Nagayama K. (2017) Extended rice-walsh equation of state for metals based on shock hugoniot data for porous samples. *J. Appl. Phys.* **121**, 175902.

Nakajima M. and Stevenson D. J. (2015) Melting and mixing states of the earth's mantle after the moon-forming impact. *Earth Planet. Sci. Lett.* **427**, 286–295.

O'Rourke J. G. (2020) Venus: A thick basal magma ocean may exist today. *Geophys. Res. Lett.* **47**, e2019GL086126.

Peng, X. c., Xing, L. l., Fang, Z. h. (2007). Comparing research on the pressure or volume dependence of Grüneisen parameter. Physica B 394, 111–114.

Plimpton S. (1995) Fast parallel algorithms for short-range molecular dynamics. *J. Comput. Phys.* **117**, 1–19.

Rigden S., Ahrens T. J. and Stolper E. (1988) Shock compression of molten silicate: results for a model basaltic composition. *J. Geophys. Res. B: Solid Earth* **93**, 367–382.

Rigden S. M., Ahrens T. J. and Stolper E. M. (1984) Densities of liquid silicates at high pressures. *Science* **226**, 1071–1074.

Shanker J., Singh B. and Baghel H. (2007) Volume dependence of the Grüneisen parameter and maximum compression limit for iron. *Phys. B* **387**, 409–414.

Shanno D. F. (1970) Conditioning of quasi-newton methods for function minimization. *Math. Comput.* **24**, 647–656.

Spera F. J., Ghiorso M. and Nevins D. (2011) Structure, thermodynamic and transport properties of liquid $MgSiO_3$: Comparison of molecular models and laboratory results. *Geochim. Cosmochim. Acta* **75**, 1272–1296.

Spera F. J., Nevins D., Ghiorso M. and Cutler I. (2009) Structure, thermodynamic and transport properties of $CaAl_2Si_2O_8$ liquid. part I: Molecular dynamics simulations. *Geochim. Cosmochim. Acta* **73**, 6918–6936.

Stixrude L. and Karki B. (2005) Structure and freezing of $MgSiO_3$ liquid in earth's lower mantle. *Science* **310**, 297–299.

Stixrude L., de Koker N., Sun N., Mookherjee M. and Karki B. B. (2009) Thermodynamics of silicate liquids in the deep earth. *Earth Planet. Sci. Lett.* **278**, 226–232.

Thomas C. W. and Asimow P. D. (2013) Direct shock compression experiments on premolten forsterite and progress toward a consistent high-pressure equation of state for CaO-MgO-Al_2O_3-SiO_2-FeO liquids. *J. Geophys. Res. B: Solid Earth* **118**, 5738–5752.

Tonks W. B. and Melosh H. J. (1993) Magma ocean formation due to giant impacts. *J. Geophys. Res. E: Planets* **98**, 5319–5333.

Trønnes R. G., Baron M. A., Eigenmann K. R., Guren M. G., Heyn B. H., Løken A. and Mohn C. E. (2019) Core formation, mantle differentiation and core-mantle interaction within earth and the terrestrial planets. *Tectonophysics* **760**, 165–198.

de Vries J., Nimmo F., Melosh H. J., Jacobson S. A., Morbidelli A. and Rubie D. C. (2016) Impact-induced melting during accretion of the earth. *Prog. Earth Planet. Sci.* **3**, 1–11.

Wolf A. S., Asimow P. D. and Stevenson D. J. (2015) Coordinated hard sphere mixture (chasm): A simplified model for oxide and silicate melts at mantle pressures and temperatures. *Geochim. Cosmochim. Acta* **163**, 40–58.

Zhang X., Sun S., Xu T. and Zhang T. (2019) Temperature dependent Grüneisen parameter. *Sci. China Technol. Sci.* **62**, 1565–1576.

Associate editor: James Van Orman